Measurement of the Electric Form Factor of the Neutron through $\vec{d}(\vec{e}, e'n)p$ at $Q^2 = 0.5\ (\mathrm{GeV}/c)^2$

H. Zhu,[1] A. Ahmidouch,[2,3] H. Anklin,[4,3] H. Arenhövel,[5] C. Armstrong,[3] C. Bernet,[6] W. Boeglin,[4,3] H. Breuer,[7] P. Brindza,[3] D. Brown,[7] S. Bültmann,[1] R. Carlini,[3] N. Chant,[7] A. Cowley,[7,3,*] D. Crabb,[1] S. Danagoulian,[2,3] D. B. Day,[1] T. Eden,[8] R. Ent,[3] Y. Farah,[2] R. Fatemi,[1] K. Garrow,[3] C. Harris,[1] M. Hauger,[6] A. Honegger,[6] J. Jourdan,[6] M. Kaufmann,[6] M. Khandaker,[8] G. Kubon,[6] J. Lichtenstadt,[9] R. Lindgren,[1] R. Lourie,[10] A. Lung,[3] D. Mack,[3] S. Malik,[9] P. Markowitz,[4,3] K. McFarlane,[8] P. McKee,[1] D. McNulty,[1] G. Milanovich,[1] J. Mitchell,[3] H. Mkrtchyan,[11] M. Mühlbauer,[6] T. Petitjean,[6] Y. Prok,[1] D. Rohe,[6] E. Rollinde,[7] O. A. Rondon,[1] P. Roos,[7] R. Sawafta,[2] I. Sick,[6] C. Smith,[1] T. Southern,[2] M. Steinacher,[6] S. Stepanyan,[11] V. Tadevosyan,[11] R. Tieulent,[7] A. Tobias,[1] W. Vulcan,[3] G. Warren,[6] H. Wöhrle,[6] S. Wood,[3] C. Yan,[3] M. Zeier,[1] J. Zhao,[6] and B. Zihlmann[1]

[1]*Institute of Nuclear and Particle Physics, University of Virginia, Charlottesville, Virginia 22903*
[2]*North Carolina A&T State University, Greensboro, North Carolina 27411*
[3]*Thomas Jefferson National Accelerator Facility, Newport News, Virginia 23606*
[4]*Florida International University, Miami, Florida 33199*
[5]*Institut für Kernphysik, Johannes Gutenberg-Universität, D-55099 Mainz, Germany*
[6]*Universität Basel, CH-4056 Basel, Switzerland*
[7]*University of Maryland, College Park, Maryland 20742*
[8]*Norfolk State University, Norfolk, Virginia 23504*
[9]*School of Physics and Astronomy, Tel Aviv University, Tel Aviv, 69978 Israel*
[10]*State University of New York, Stonybrook, New York 11794*
[11]*Yerevan Physics Institute, Yerevan, Armenia*
(Received 26 March 2001; published 3 August 2001)

We report the first measurement using a solid polarized target of the neutron electric form factor G_E^n via $\vec{d}(\vec{e}, e'n)p$. G_E^n was determined from the beam-target asymmetry in the scattering of longitudinally polarized electrons from polarized deuterated ammonia ($^{15}\mathrm{ND}_3$). The measurement was performed in Hall C at Thomas Jefferson National Accelerator Facility in quasifree kinematics with the target polarization perpendicular to the momentum transfer. The electrons were detected in a magnetic spectrometer in coincidence with neutrons in a large solid angle segmented detector. We find $G_E^n = 0.04632 \pm 0.00616(\mathrm{stat}) \pm 0.00341(\mathrm{syst})$ at $Q^2 = 0.495\ (\mathrm{GeV}/c)^2$.

DOI: 10.1103/PhysRevLett.87.081801 PACS numbers: 13.40.Gp, 14.20.Dh

Precise data on the neutron (and proton) form factors are important for understanding the nonperturbative mechanism responsible for confinement and are necessary in the interpretation of the electromagnetic properties of nuclei. The magnetic form factor of the neutron [1] has been measured with high precision. The neutron charge form factor G_E^n, in contrast, is only now yielding to intense efforts focused on its determination.

The major difficulty faced in a measurement of the neutron form factors is the lack of a free neutron target. The determination of G_E^n is further impeded by its small size. Advances in polarized-electron sources, high duty factor accelerators, polarimeters, and polarized targets now allow G_E^n to be extracted from experiments which exploit spin degrees of freedom. In particular the interference of the magnetic and electric scattering amplitudes is responsible for an asymmetry that can be measured in both polarized-electron–polarized-target experiments [$\vec{d}(\vec{e}, e'n)p$ [2] and $^3\vec{\mathrm{He}}(\vec{e}, e'n)p$ [3–5]] and in polarized-electron recoil polarization measurements [$d(\vec{e}, e'\vec{n})p$ [6–8]].

For a vector polarized target of free neutrons, with the polarization P_n, in the scattering plane and perpendicular to the momentum transfer $\vec{q}$, G_E^n is related to the helicity asymmetry A_{en}^V [9] by

$$A_{en}^V = \frac{-2\sqrt{\tau(\tau + 1)}\tan(\theta_e/2)G_E^n G_M^n}{(G_E^n)^2 + \tau[1 + 2(1 + \tau)\tan^2(\theta_e/2)](G_M^n)^2}, \tag{1}$$

where Q^2 is the four-momentum transfer, $\tau = Q^2/4M_n^2$, and θ_e is the electron scattering angle. A_{en}^V is related to the experimental count asymmetry $\epsilon = (L - R)/(L + R)$, where L and R are charge normalized counts for opposite beam polarizations P_e, by $A_{en}^V = \epsilon/(P_e P_n f)$, where f is the dilution factor due to scattering from materials other than polarized neutrons.

In practice, one measures the helicity asymmetry from polarized deuterons in quasielastic kinematics. The count asymmetry for polarized-electron, polarized-deuteron scattering can be written, following [10,11], as

$$\epsilon = f\,\frac{P_e A_e + P_e P_1^d A_{ed}^V + P_e P_2^d A_{ed}^T}{1 + P_1^d A_d^V + P_2^d A_d^T}, \tag{2}$$

where $P_{1(2)}^d$ is the target vector (tensor) polarization, and A_e, A_d^V, A_d^T, A_{ed}^V, and A_{ed}^T are the electron beam induced asymmetry, the vector and tensor deuteron target asymmetries, and the deuteron vector and tensor beam-target asymmetries, respectively. For experiments with the target polarization in the scattering plane which sample the neutron Fermi cone in an azimuthally symmetric way this reduces to

$$\epsilon = f \frac{P_e P_1^d A_{ed}^V}{1 + P_2^d A_d^T}. \tag{3}$$

For most practical targets P_2^d is small (3%) and the second term in the denominator may be neglected. Realistic calculations indicate that A_{ed}^V has a linear sensitivity to the magnitude of G_E^n for $d(e, e'n)$ at low recoil momentum [10,11].

We present in this Letter a measurement at $Q^2 = 0.495$ $(\mathrm{GeV}/c)^2$ carried out at Thomas Jefferson National Accelerator Facility (TJNAF) in Hall C. A longitudinally polarized electron beam of 2.725 GeV incident energy and $\approx$100 nA beam current scattered off a dynamically polarized solid deuterated ammonia target. The scattered electrons were detected in coincidence with the knockout neutrons.

The polarized-electron beam was produced by photoemission from a strained-layer semiconductor cathode illuminated by circularly polarized laser light [12] at the accelerator injector. The helicity of the beam was changed in a pairwise pseudorandom sequence once per second to minimize sensitivity to instrumental drifts. The longitudinal polarization of the electrons was measured at regular intervals during the experiment with a Møller polarimeter [13] just upstream of the target. The average beam polarization for the data taking was $P_e = 0.776 \pm 0.002(\mathrm{stat})$.

To prevent localized heating of the target material and to ensure uniform irradiation, the beam was rastered over the face of the target such that the full face of the target was illuminated during each helicity state. The beam position was recorded by a secondary emission monitor [14] consisting of thin stainless steel strips in both the horizontal and vertical directions.

The polarized target [15] included a permeable target cell filled with granules of $^{15}ND_3$ submerged in liquid He maintained at 1 K by a high power He evaporation refrigerator. A 5 T magnetic field was provided by a superconducting coil arranged as a Helmholtz pair. The magnetic field was in the horizontal plane perpendicular to $\langle \vec{q} \rangle$ at 151.6° with respect to the beam direction. The field orientation was measured *in situ* with a Hall probe to $\pm 0.1°$. A three-magnet chicane compensated for the effects of the target magnetic field on the incident electrons. The field effects on the scattered electrons tilted the scattering plane by 4° with respect to the horizontal plane. The target material was polarized by the dynamic nuclear polarization method. The polarization was measured continuously via NMR using a series *LCR* circuit and *Q* meter detector [16]. The average deuteron polarization throughout the experiment was $P_1^d = 0.21 \pm 0.01$.

The high momentum spectrometer (HMS) in its standard configuration was set at 15.7° to detect the scattered electrons. Modifications were made to the standard reconstruction algorithm of the HMS to account for the target field and the beam raster offset.

Knockout nucleons (p and n) were detected in an array of plastic scintillators. It consisted of two planes of thin (0.6 cm) veto paddles and five planes of 10-cm-thick bars. The scintillator bars (160-cm long in the horizontal direction) had a phototube at each end to allow good position and timing resolution. The detector was positioned at 61.6° (along the direction of $\langle \vec{q} \rangle$), providing a solid angle of $\approx$160 msr and was enclosed in a thick concrete walled hut open towards the target. The front shielding consisted of 16.7 mm of lead and 25 mm of CH_2 sheets. The time resolution was 450 ps (σ) as determined from the time-of-flight peak of photons (from π^0 decay) in the mean time spectrum. With the detector positioned 4.2 m from the target it provided an energy resolution of 16.5 MeV for nucleons with a kinetic energy of 267 MeV. Knowledge of the neutron energy combined with the scattered electron energy allowed us to eliminate events associated with pion production. The neutron vertical position was determined by the segmentation of the detector (10 cm) while the horizontal position was determined from the time difference of the phototubes on the first bar hit along the n track. The measured horizontal resolution was $\approx$5 cm.

The electron-nucleon trigger was formed by a coincidence between the HMS electron and a hit in any one of the veto or bar planes. Neutrons were identified as events with no hits in the paddles along the track to the target, within a narrow time interval, and in a narrow range of invariant mass W around the nucleon mass ($|W - 939\ \mathrm{MeV}| < 50$ MeV). In addition, cuts on the horizontal position ($|y_{\mathrm{pos}}| < 40$ cm) in the neutron detector and on the angle between $\vec{q}$ and the neutron momentum ($\theta_{nq} < 110$ mrad) were applied to optimize the dilution factor. The θ_{nq} cut also served to limit the recoil momentum p_r to values where the model dependence of A_{ed}^V has been shown to be small ($p_r^{\max} \approx 85\ \mathrm{MeV}/c$) [10]. The protons were bent vertically in the target field by nearly 18°, almost eliminating their overlap with the neutrons and further improving their rejection.

The experimental asymmetry was diluted by scattering from materials other than polarized deuterium nuclei. These include the nitrogen in $^{15}ND_3$, the liquid helium, the NMR coils, and target windows. A Monte Carlo (MC) simulation program was developed [17] to determine the dilution factor and to perform the detector averaging of the theoretical asymmetries. It was based on MCEEP [18] and included a model of the HMS, the neutron detector geometry and approximate efficiencies, the target magnetic field, the beam raster, and radiative effects. Quasielastic scattering from all the target materials was simulated in the MC. The normalization was fixed by data from carbon (which approximates nitrogen) and liquid helium. A comparison of the simulated distributions to experimental data is shown in Fig. 1 for four kinematic variables. The good agreement of the distributions indicates that quasielastic scattering is the dominant process for events passing our selection criteria.

The accidental background under the mean time distribution was 4% and had no statistically significant asymmetry. The measured asymmetry was corrected for this dilution. A correction of 0.2% was made for the proton contamination. Charge exchange in deuterium was taken into account in the theoretical calculations of final state interactions (FSI). No correction was applied for charge exchange reactions with other target materials or the shielding (estimated to be 0.24%). The role of radiative effects on A_{ed}^V was estimated and found to be small. Corrections to the asymmetry for internal radiative effects of 2% and 0.5% for external effects were applied.

In order to extract G_E^n, the corrected experimental asymmetry was compared to the MC simulation in which theoretical calculations of the asymmetry are weighted by the event distribution. The theoretical asymmetries were calculated on a grid reflecting our experimental arrangement under different assumptions for the size of G_E^n. Asymmetry values between grid points were obtained by interpolation.

The theoretical A_{ed}^V values were calculated following [10,11]. The calculations are based on a nonrelativistic description of the n-p system in the deuteron, using the Bonn R-space NN potential [19] for both the bound state and the description of FSI. The full calculations include meson exchange currents and isobar configurations as well as relativistic corrections. The dipole parametrization for G_M^n was assumed. It was verified that the acceptance averaged value of A_{ed}^V is linear in the size of G_M^n. Thus any (experimental) value could be incorporated easily if desired. The grid of asymmetries was calculated for three values of G_E^n. In all cases the Q^2 variation of G_E^n was assumed to be given by the Galster parametrization [20] (with $p = 5.6$) with the magnitude set by an overall scale parameter of 0.5, 1, or 1.5. The narrow acceptance in Q^2, $0.4 < Q^2 < 0.6$ $(\mathrm{GeV}/c)^2$, makes the extracted value of G_E^n insensitive to the assumed Q^2 dependence.

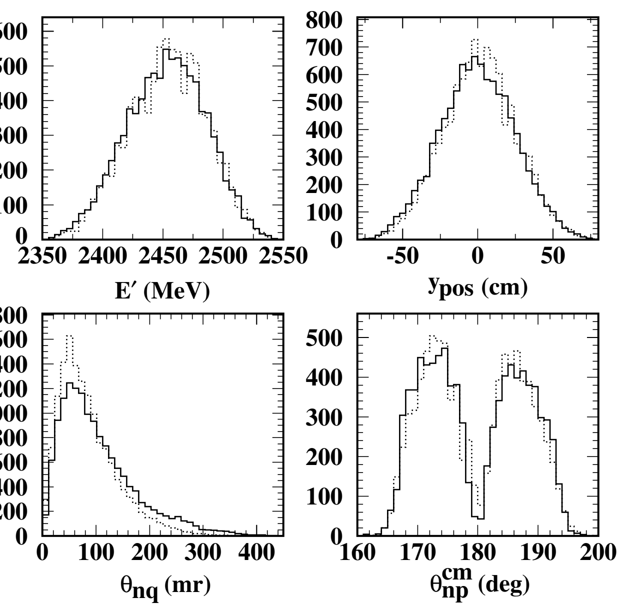

FIG. 1. A comparison between the data (solid lines) and the MC simulation (dotted lines) for $(e, e'n)$ from $^{15}ND_3$ for four kinematic variables: E' (scattered electron energy), y_{pos} (horizontal position in the neutron detector), θ_{nq} (the angle between $\vec{q}$ and the neutron in the lab), and θ_{np}^{cm} (the calculated angle between the proton and $\vec{q}$ in the n-p center of mass).

The MC simulation averaged the asymmetry over all kinematic variables except the one under investigation. The comparisons are shown in Fig. 2. To determine the best value of the scale parameter, it was fit as a free parameter to the data. The resulting value for G_E^n at $Q^2 = 0.495$ $(\mathrm{GeV}/c)^2$ is $G_E^n = 0.04632 \pm 0.00616(\mathrm{stat}) \pm 0.00341(\mathrm{syst})$.

The major sources of systematic errors are $\delta P_1^d / P_1^d = 5.8\%$, and the uncertainty in determining the average dilution factor is 3.9%. Cut dependencies give a 2.4% systematic error. Errors associated with the determination of various kinematic quantities contribute another 2.2%. The determination of P_e contributes 1%. The error in the value of G_M^n was taken to be 1.7% as derived from a recent fit to world data [21]. The quadratic sum of all the contributions gives a total systematic error $\delta G_E^n / G_E^n = 7.4\%$.

Our measurement is compared to G_E^n measurements from other polarized experiments in Fig. 3. The solid line and band represent our fit of the data set shown with the form

$$G_E^n(Q^2) = -\mu_n \frac{a\tau}{1 + p\tau} G_D(Q^2)$$

with $G_D(Q^2) = 1/(1 + Q^2/\Lambda^2)^2$ and $\Lambda^2 = 0.71$ $(\mathrm{GeV}/c)^2$.

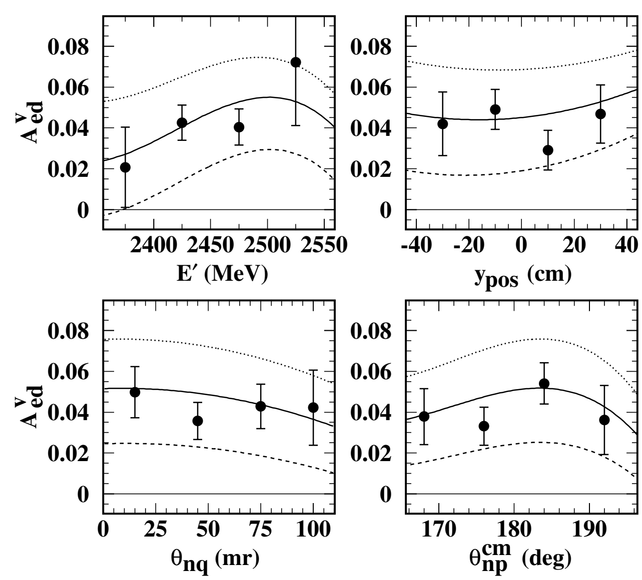

FIG. 2. Comparison between the measured asymmetries and calculated values of A_{ed}^V for three scaled Galster parametrizations [0.5 (dashed lines), 1.0 (solid lines), 1.5 (dotted lines)] shown against four kinematic variables.

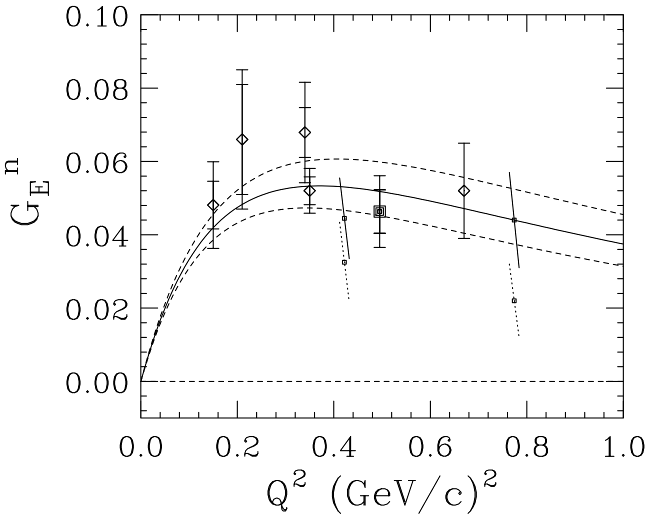

FIG. 3. Comparison of this experiment (filled square) with data from recent polarized scattering measurements, from left to right [7], [2], [8], [4], and [3]. FSI corrections have been made for all the data except [3], where FSI are thought to be modest. Data from Ref. [4] were corrected for FSI [24]. The solid line and band represent our fit of this data set (see text). The slanted lines are lattice QCD calculations with (solid lines) and without (dotted lines) the disconnected insertions which account for sea-quark effects [23].

The parameter a is fixed by a measurement of $\frac{dG_E^n}{dQ^2}$ at $Q^2 = 0$ [22]. With $a = 0.895 \pm 0.039$ we find $p = 4.36 \pm 1.11$ for the six data points. The figure also shows the results of recent lattice QCD calculations [23]. In these calculations G_E^n is quite sensitive to the disconnected insertions which account for the sea quarks. The magnitude of these sea contributions to the various nucleon form factors is almost constant so they are relatively much more important for G_E^n. Thus G_E^n may provide a valuable testing ground for lattice calculations of other sea sensitive quantities such as the strangeness electric and magnetic form factors.

The size of the reaction dynamic effects beyond the plane wave Born approximation (PWBA) was determined by repeating the same extraction procedure using PWBA calculations. The result for G_E^n was found to be 13% smaller than when it was extracted from A_{ed}^V using the full calculation. The bulk of the difference is due to FSI.

In conclusion we present the results of a new measurement of the neutron electric form factor at $Q^2 = 0.495$ (GeV$/c)^2$, the highest momentum transfer to date in polarized scattering using a deuteron target. This measurement sets a new constraint on the parametrizations of G_E^n and, more importantly, on theoretical models which describe it. In addition it will contribute to the extraction of strange quark form factors from parity violating (PV) elastic scattering from protons [25,26], where errors on previous measurements of G_E^n are the largest contributor to the theoretical PV asymmetry, A_{th}. The ongoing effort to measure G_E^n will considerably extend our understanding of nucleon structure.

We wish to thank the Hall C technical and engineering staffs at TJNAF as well as the injector, polarized target, FEL, and survey groups for their outstanding support. This work was supported by the Commonwealth of Virginia through the Institute of Nuclear and Particle Physics at the University of Virginia, the Schweizerische Nationalfonds, by DOE Contract No. DE-FG02-96ER40950 (University of Virginia), the U.S.-Israel Binational Science Foundation (Tel Aviv University), and by Deutsche Forschungsgemeinshaft (SFB 443). The Southeastern Universities Research Association (SURA) operates the Thomas Jefferson National Accelerator Facility for the United States Department of Energy under Contract No. DE-AC05-84ER40150.

*Permanent address: Department of Physics, University of Stellenbosch, Private Bag X1, Matieland, 7602, South Africa.

[1] H. Anklin *et al.,* Phys. Lett. B **336**, 313 (1994); H. Anklin *et al.,* Phys. Lett. B **428**, 248 (1998).
[2] I. Passchier *et al.,* Phys. Rev. Lett. **82**, 4988 (1999).
[3] D. Rohe *et al.,* Phys. Rev. Lett. **83**, 4257 (1999).
[4] J. Becker *et al.,* Eur. Phys. J. A **6**, 329 (1999).
[5] M. Meyerhoff *et al.,* Phys. Lett. B **327**, 201 (1994).
[6] T. Eden *et al.,* Phys. Rev. C **50**, R1749 (1994).
[7] C. Herberg *et al.,* Eur. Phys. J. A **5**, 131 (1999).
[8] M. Ostrick *et al.,* Phys. Rev. Lett. **83**, 276 (1999).
[9] T. W. Donnelly and A. S. Raskin, Ann. Phys. (N.Y.) **169**, 247 (1986); A. S. Raskin and T. W. Donnelly, Ann. Phys. (N.Y.) **191**, 78 (1989).
[10] H. Arenhövel, W. Leidemann, and E. L. Tomusiak, Z. Phys. A **331**, 123 (1988); **334**, 363(E) (1989).
[11] H. Arenhövel, W. Leidemann, and E. L. Tomusiak, Phys. Rev. C **46**, 455 (1992).
[12] C. Sinclair, TJNAF Report No. TJNAF-TN-97-021.
[13] M. Hauger *et al.,* Nucl. Instrum. Methods Phys. Res., Sect. A **462**, 382 (2001).
[14] M. Steinacher and I. Sick, Nucl. Instrum. Methods Phys. Res., Sect. A **455**, 759 (2000).
[15] D. Crabb and D. Day, Nucl. Instrum. Methods Phys. Res., Sect. A **356**, 9 (1995); T. D. Averett *et al.,* Nucl. Instrum. Methods Phys. Res., Sect. A **427**, 440 (1999).
[16] G. Court, Nucl. Instrum. Methods Phys. Res., Sect. A **324**, 443 (1993).
[17] H. Zhu, Ph.D. thesis, University of Virginia, 2000. Details of the analysis can be found therein.
[18] P. Ulmer, MCEEP, Version 3.3, 2000.
[19] R. Machleidt, K. Holinde, and Ch. Elster, Phys. Rep. **149**, 1 (1987).
[20] S. Galster *et al.,* Nucl. Phys. **B32**, 221 (1971).
[21] J. Jourdan, Proceedings of the XVIIth European Conference on Few-Body Problems in Physics, Évora, 2000.
[22] S. Kopecky *et al.,* Phys. Rev. Lett. **74**, 2427 (1995).
[23] S. J. Dong, K. F. Liu, and A. G. Williams, Phys. Rev. D **58**, 074504 (1998); K. F. Liu (private communication).
[24] J. Golak *et al.,* Phys. Rev. C **63**, 034006 (2001).
[25] K. A. Aniol *et al.,* Phys. Rev. Lett. **82**, 1096 (1999).
[26] K. A. Aniol *et al.,* nucl-ex/0006002.